

# Scintillation Properties of Nd-doped LuVO<sub>4</sub> Single Crystals

Masaki Akatsuka,\* Nakauchi Daisuke, Kato Takumi,  
Noriaki Kawaguchi, and Takayuki Yanagida

Division of Materials and Science, Nara Institute of Science and Technology,  
8916-5, Takayama, Ikoma, Nara 630-0192, Japan

(Received October 15, 2021; accepted November 25, 2021)

**Keywords:** scintillator, near-infrared, single crystals, high-dose monitoring

Nd-doped LuVO<sub>4</sub> single crystals were synthesized by the floating zone method and their optical properties including scintillation were evaluated. The synthesized Nd-doped LuVO<sub>4</sub> samples had a LuVO<sub>4</sub> single phase. The 1.0% Nd-doped LuVO<sub>4</sub> had the highest photoluminescence (PL) quantum yield (87%) of all the samples in the NIR range. The Nd-doped LuVO<sub>4</sub> samples showed scintillation peaks around 900, 1060, and 1320 nm due to the electronic transition of Nd<sup>3+</sup>. Moreover, there was a strong correlation between the scintillation signal intensity and the X-ray exposure dose rate in the wavelength range from 900 to 1600 nm, and all the samples showed good linearity with a dynamic range from 0.006 to 60 Gy/h.

## 1. Introduction

A scintillator is a fluorescent material that converts the absorbed energy of radiation into a large number of UV–NIR photons.<sup>(1)</sup> The range of applications of scintillators is very wide, including the fields of medicine,<sup>(2)</sup> high-energy physics,<sup>(3)</sup> environmental monitoring,<sup>(4)</sup> and security.<sup>(5)</sup> Although scintillators require various characteristics depending on the application, for example, high light yield, fast decay time, high atomic number, and chemical stability,<sup>(6,7)</sup> no perfect scintillators that satisfy all these requirements have been found. Thus, appropriate scintillators are selected according to the purpose, and various types of scintillators have been developed, such as liquid,<sup>(8,9)</sup> plastic,<sup>(10,11)</sup> inorganic/organic,<sup>(12,13)</sup> glass,<sup>(14,15)</sup> ceramic,<sup>(16,17)</sup> and single-crystal scintillators.<sup>(18,19)</sup>

Recently, scintillators emitting NIR photons have attracted considerable interest because of their unique properties. For example, since the optical transmission window of biological tissues of 700–1200 nm allows deeper light penetration, lower autofluorescence, and reduced light scattering,<sup>(20–23)</sup> NIR photons are more suitable for biomedical applications. Possible biomedical applications are real-time monitoring of the irradiation field during radiation therapies and their combined use with photoimmunotherapy. In such applications, a very small scintillator emitting NIR photons is expected to be embedded in a patients body.

---

\*Corresponding author: e-mail: [akatsuka.masaki.ad5@ms.naist.jp](mailto:akatsuka.masaki.ad5@ms.naist.jp)  
<https://doi.org/10.18494/SAM3692>

Moreover, scintillators emitting NIR photons are expected to be an effective tool for high-dose monitoring. In high-dose environments, Cherenkov photons often appear and overlap with the scintillation signal, which is in the UV–blue range.<sup>(24,25)</sup> However, scintillators emitting NIR photons can be used because NIR photons are easily separated from Cherenkov photons.

Although scintillators emitting NIR photons have advantages over those emitting UV–VIS photons, there have been few studies of NIR-emitting scintillators. This is because conventional photodetectors are sensitive to UV and visible photons. Thus, studies have generally been on scintillators emitting UV or visible photons, and there remains much room for the study of scintillators emitting NIR photons.

Recently, our group has overcome this issue by using InGaAs-based photodetectors sensitive to wavelengths in the NIR range; thus, we have been studying NIR-emitting scintillators.<sup>(26–33)</sup> In particular, vanadate crystals tend to exhibit high scintillation efficiency in the NIR range. In this study, we prepared Nd-doped LuVO<sub>4</sub> single crystals by the floating zone (FZ) method and evaluated their photoluminescence (PL) and X-ray-induced scintillation properties. The effective atomic number  $Z_{eff}$  of LuVO<sub>4</sub> is 62.3, comparable to that of conventional scintillators such as GSO<sup>(34)</sup> and LuAG.<sup>(35)</sup> Moreover, LuVO<sub>4</sub> is a well-known phosphor and laser material,<sup>(36,37)</sup> and the scintillation properties of non-doped LuVO<sub>4</sub> have already been studied.<sup>(38)</sup> However, to our knowledge, Nd-doped LuVO<sub>4</sub> has not been evaluated as an NIR scintillator.

## 2. Materials and Methods

Nd-doped LuVO<sub>4</sub> single crystals were synthesized as follows. Powders of Lu<sub>2</sub>O<sub>3</sub> (5N, Nippon Yttrium), V<sub>2</sub>O<sub>5</sub> (4N, High Purity Chemical), and Nd<sub>2</sub>O<sub>3</sub> (4N, Rare Metallic) were mixed in a stoichiometric ratio. Here, the Nd concentrations were 0, 0.1, 0.3, 1.0, 3.0, and 10%, where Nd<sup>3+</sup> replaced Lu<sup>3+</sup>. The mixture was calcined at 800 °C for 12 h in air and the calcined mixture was ground for the preparation of ceramic rods. A rubber tube was filled with the ground powder using an infundibulum, then the tube was shaped into a rod by hydrostatic pressure. The pressed rod was sintered at 1100 °C for 8 h in air. The obtained rod was grown into a single crystal by the FZ method using a process described in previous studies.<sup>(39,40)</sup> Powder X-ray crystallography of the sample was performed using an X-ray diffractometer (Miniflex 600, Rigaku) in the  $2\theta$  range of 5–90°.

To investigate the optical properties of the single crystals, we evaluated the diffuse transmittance spectra using a UV–VIS–NIR spectrophotometer (SolidSpec-3700, SHIMADZU) in the spectral range from 200 to 900 nm with 1 nm steps. The PL excitation/emission contour spectrum (PL map) and PL quantum yield ( $QY$ ) were evaluated using a Quantaaurus-QYplus spectrometer (C13534, Hamamatsu). The excitation and emission wavelength ranges for the PL map were 250–800 and 300–1600 nm, respectively. PL decay time profiles were obtained using a Quantaaurus- $\tau$  spectrometer (C11367, Hamamatsu), where the excitation and monitoring wavelengths were 575–625 nm and 810 nm, respectively.

Scintillation spectra were measured with an X-ray generator (XRB80N100/CB, Spellman) and spectrometers (Andor DU-420-BU2 CCD and Andor DU492A CCD with spectral sensitivities of 200–700 nm and 700–1600 nm, respectively). The setup of this measurement

system was reported previously.<sup>(41,42)</sup> Scintillation decay time profiles were measured with an LED, an X-ray tube (N-5084), and a photomultiplier tube (PMT) (Hamamatsu, H7421-50). The setups of these measurements were reported in a previous study.<sup>(43)</sup> In addition, to determine the detector properties of the Nd-doped LuVO<sub>4</sub> samples, the relationship between the scintillation signal intensity and X-ray exposure dose rate was measured by applying our original setup.<sup>(26,27)</sup> The samples were broken into pieces and used for this measurement. The size of each sample was about  $5 \times 5 \times 3 \text{ mm}^3$ . The prepared samples were covered with sealing tape to detect the scintillation light effectively and were fixed to an optical fiber using black tape.

### 3. Results and Discussion

The obtained crystal samples had 4 mm diameter and 15 mm length, and the samples were broken into pieces for each measurement. A photograph of the samples is shown in Fig. 1. The 1.0, 3.0, and 10% Nd-doped LuVO<sub>4</sub> samples were purple, which is considered to be due to the presence of Nd<sup>3+</sup>.

The powder XRD patterns of all the samples and LuVO<sub>4</sub> as reference data (Powder Diffraction File #9013518) are shown in Fig. 2(a), and enlarged diffraction patterns from 24.5 to

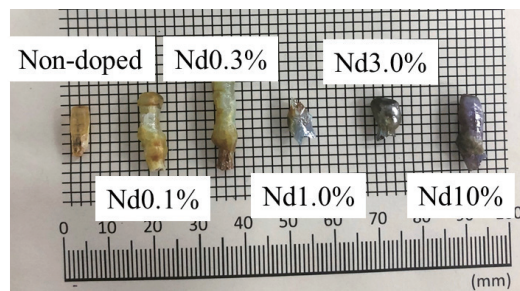


Fig. 1. (Color online) Photograph of the samples.

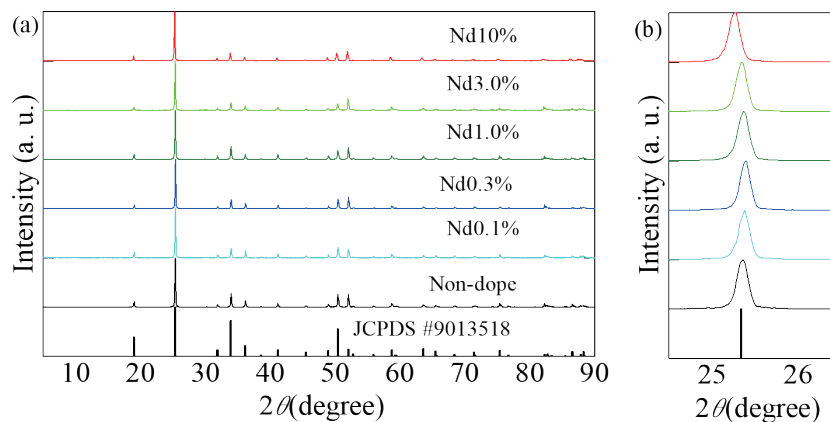


Fig. 2. (Color online) (a) Powder XRD patterns of LuVO<sub>4</sub> samples and (b) enlarged figure in the range from 24.5 to 26.5°.

26.5° are shown in Fig. 2(b). The diffraction patterns of all the samples were coincident with the reference data, and the crystal structure of the samples was confirmed to be the zircon-type structure, which belongs to the  $I4_1/amd$  space group of a tetragonal crystal system. As shown in Fig. 2(b), the diffraction peaks shifted to smaller angles with increasing Nd/Lu ratio. The ionic radius of Nd is 1.109 Å and that of Lu is 0.977 Å. Our result is consistent with the fact that when the lattice constant decreases, the diffraction peaks shift to smaller angles.

Figure 3 shows the diffuse transmittance spectra of all the samples in the wavelength range of 200–850 nm. The transmittance of all the samples was 20–70% for wavelengths longer than about 350 nm. The Nd-doped samples showed absorption peaks due to the 4f–4f transition of  $Nd^{3+}$ .

Figure 4 shows PL maps of the (a) non-doped sample and (b) 0.1% Nd-doped sample. The other Nd-doped samples also exhibited the same emission features. The PL map of the non-doped sample showed emission around 400–600 nm due to the transition from triplet states of  $VO_4^{3-}$ .<sup>(44,45)</sup> As shown in Fig. 4(b), emissions around 900, 1060, and 1320 nm due to the 4f–4f transitions of  $Nd^{3+}$  were observed.<sup>(46–48)</sup> The  $QY$  values of Nd-doped  $LuVO_4$  were calculated from 800 to 1500 nm and the selected excitation wavelength was 590 nm. The  $QY$  values of the 0.1, 0.3, 1.0, 3.0, and 10% Nd-doped samples were 80.3, 86.3, 87.0, 53.1, and 20.5%, respectively; the  $QY$  values of the 0.3 and 1.0% Nd-doped samples were higher than those of the other Nd-doped samples.

The PL decay time profiles of the Nd-doped  $LuVO_4$  samples were measured from the obtained PL map, and the result is shown in Fig. 5. Here, the excitation and monitoring wavelengths were 575–625 nm and 800 nm, respectively. Each obtained PL decay curve indicated the simple exponential decay of a single component. The PL decay time constants of the 0.1–10% Nd-doped samples were 11.5–88.5  $\mu s$ , which are typical values for emission from 4f–4f transitions of  $Nd^{3+}$  and agree with the values reported in past studies.<sup>(49,50)</sup> On the other hand, the 3.0 and 10% Nd-doped samples have very short decay time constants. This finding suggests that these samples suffered from concentration quenching.

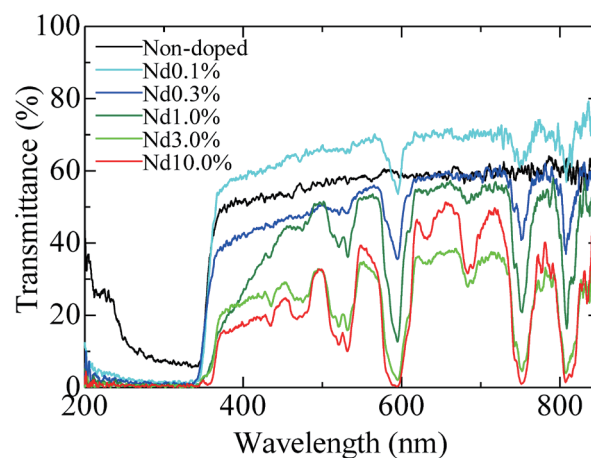


Fig. 3. (Color online) Diffuse transmittance spectra of all the samples.

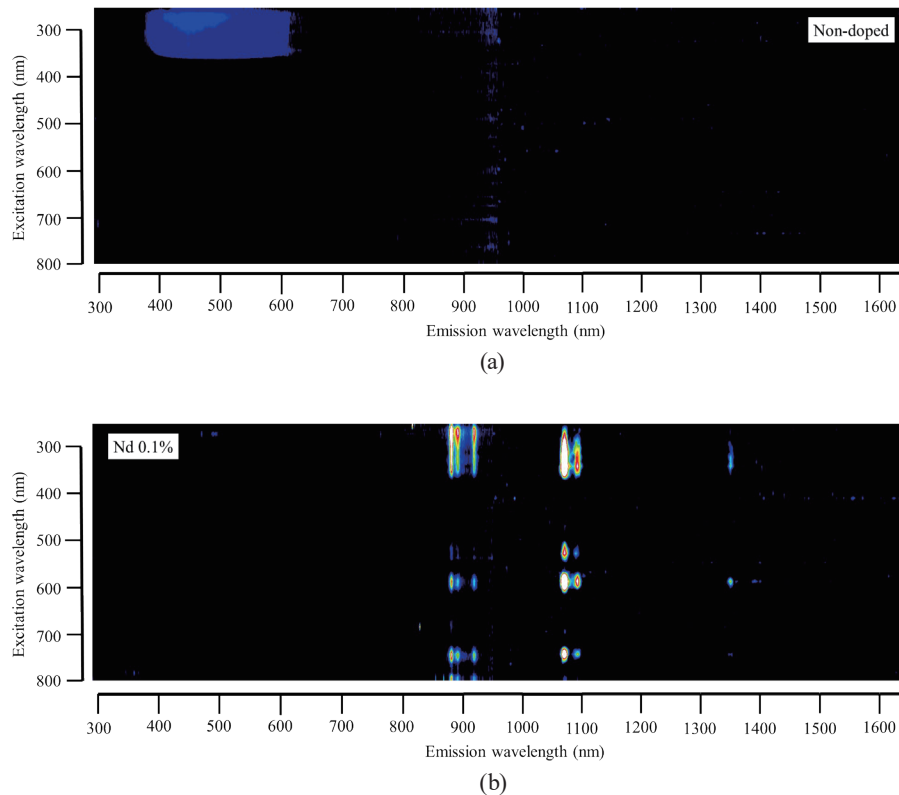


Fig. 4. (Color online) PL maps of (a) non-doped  $\text{LuVO}_4$  sample and (b) 0.1% Nd-doped  $\text{LuVO}_4$  as a representative Nd-doped sample. The vertical and horizontal axes show the excitation wavelength and emission wavelength, respectively.

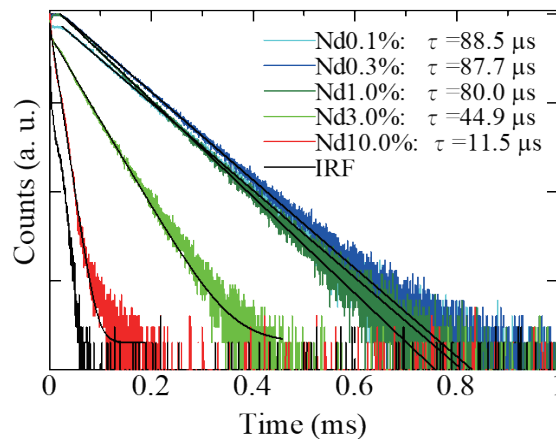


Fig. 5. (Color online) PL decay curves of Nd-doped  $\text{LuVO}_4$  samples.

Figure 6 shows X-ray-induced scintillation spectra of the samples measured in the (a) UV–VIS and (b) NIR ranges. In the UV–VIS range, the non-doped, 0.1%, and 0.3% Nd-doped samples showed emission around 400–500 nm due to the transition from triplet states of  $\text{VO}_4^{3-}$ . The spectra of the 0.1 and 0.3% Nd-doped samples showed absorption bands about 520 and

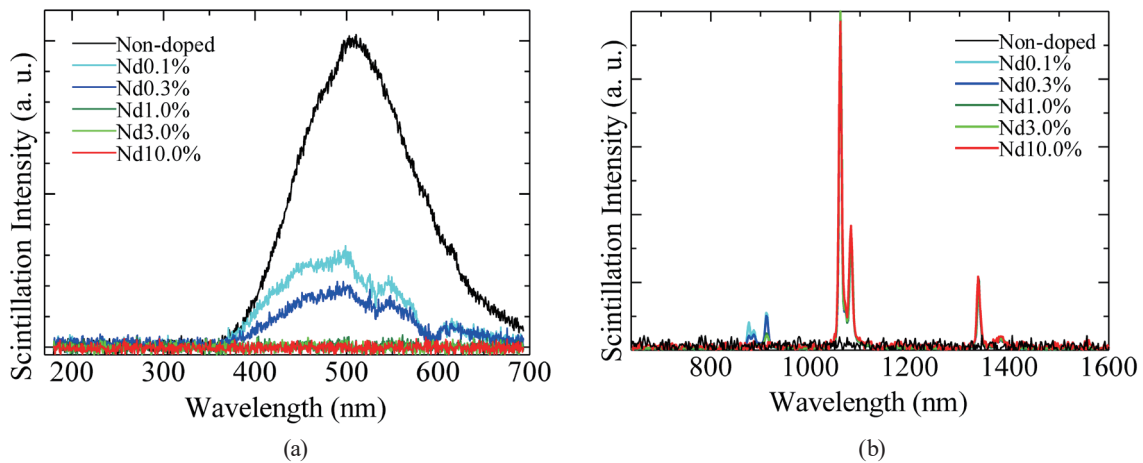


Fig. 6. (Color online) Scintillation spectra of all the LuVO<sub>4</sub> samples in (a) UV–VIS and (b) NIR ranges.

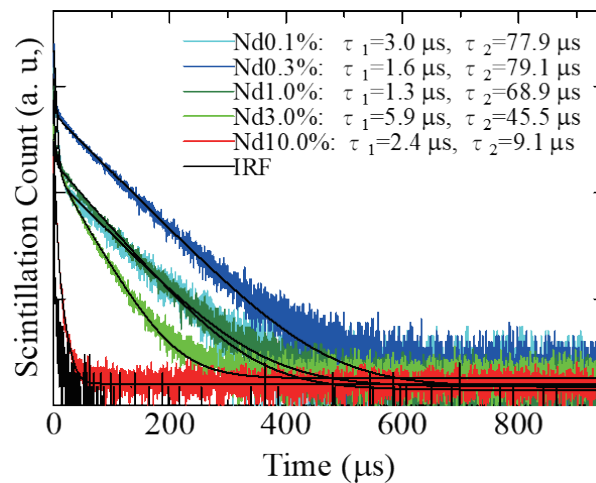


Fig. 7. (Color online) Scintillation decay curve of Nd-doped LuVO<sub>4</sub> samples.

600 nm, corresponding to the observed diffuse transmittance of the samples. In the NIR range, all the Nd-doped samples exhibited emissions due to the electronic transitions of Nd<sup>3+</sup>  $^4F_{3/2} \rightarrow ^4I_{9/2}$  (910 nm),  $^4F_{3/2} \rightarrow ^4I_{11/2}$  (1060 nm), and  $^4F_{3/2} \rightarrow ^4I_{13/2}$  (1320 nm).<sup>(51,52)</sup> Moreover, the Nd-doped samples did not exhibit emission due to the 4f–4f transition of Nd<sup>3+</sup> in the UV–VIS range. For example, in a past study, it was reported that Nd-doped GdVO<sub>4</sub> exhibits energy transfer from VO<sub>4</sub><sup>3-</sup> ions to the  $^4F_{3/2}$  level.<sup>(53)</sup> The radiative transitions from the  $^4F_{3/2}$  levels to the  $^4I_{9/2}$ ,  $^4I_{11/2}$ , and  $^4I_{13/2}$  energy levels of Nd<sup>3+</sup> ions generate the 900, 1060, and 1320 nm NIR emissions, respectively. Since LuVO<sub>4</sub> is similar to GdVO<sub>4</sub>, the Nd-doped LuVO<sub>4</sub> samples are expected to emit light in the NIR range with high efficiency.

Figure 7 shows X-ray-induced scintillation decay time profiles of the Nd-doped LuVO<sub>4</sub> samples. The decay curves of all the Nd-doped samples were approximated as a sum of two exponential decay functions, and the faster decay components were considered to correspond to the tail of the instrumental response (1.3–5.9 μs) in this time range. The slower decay components

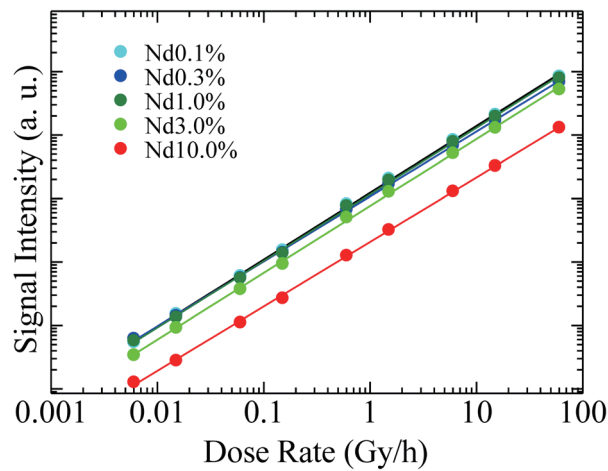


Fig. 8. (Color online) Relationship between scintillation intensity and X-ray exposure dose rate from 0.006 to 60 Gy/h.

were considered to be due to the 4f–4f transitions of  $\text{Nd}^{3+}$  because they were typical values for the 4f–4f transitions of  $\text{Nd}^{3+}$  reported in past studies.<sup>(27,54)</sup> The slower components of the 3.0 and 10% Nd-doped samples were shorter than those of the other Nd-doped samples, similarly to in the PL decay time profiles.

To determine the dosimetric detector properties of the samples, we evaluated the correlation between the scintillation signal intensity and the exposure dose rate of X-rays, and the obtained results are shown in Fig. 8. Here, the scintillation wavelength was 900 to 1700 nm and the dose rate range was from 0.006 to 60 Gy/h. All the Nd-doped samples indicated high sensitivity in the dynamic range from 0.006 to 60 Gy/h. This result is comparable to those of Nd-doped  $\text{GdVO}_4$ , which had the highest sensitivity to low dose rates among the past studies.

#### 4. Conclusion

We prepared Nd-doped  $\text{LuVO}_4$  single crystals. All the Nd-doped samples showed emissions around 900, 1060, and 1320 nm according to the PL map and X-ray-induced scintillation spectra owing to the 4f–4f transitions of  $\text{Nd}^{3+}$  ions. The PL decay times of the Nd-doped samples were 11.5–88.5  $\mu\text{s}$  and the scintillation decay times of the Nd-doped samples were 9.1–79.1  $\mu\text{s}$ . The relationship between the scintillation signal intensity and the exposure dose rate of X-rays was estimated from 0.006 to 60 Gy/h in the NIR range, and all the Nd-doped samples exhibited good linearity from 0.006 to 60 Gy/h.

#### Acknowledgments

This work was supported by Grants-in-Aid for Scientific Research, Scientific Research B (19H03533), Early-Career Scientists (20K20104 and 20K15026), and JSPS Fellows (19J22402) from JSPS. The Cooperative Research Project of the Research Institute of Electronics, Shizuoka

University, Murata Foundation, Iketani Foundation, Nippon Sheet Glass Foundation, and NAIST Foundation are also acknowledged.

## References

- 1 T. Yanagida: Proc. Japan Acad. Ser. B. **94** (2018) 75.
- 2 T. Yanagida, A. Yoshikawa, Y. Yokota, K. Kamada, Y. Usuki, S. Yamamoto, M. Miyake, M. Baba, K. Kumagai, K. Sasaki, M. Ito, N. Abe, Y. Fujimoto, S. Maeo, Y. Furuya, H. Tanaka, A. Fukabori, T. Rodrigues dos Santos, M. Takeda, and N. Ohuchi: IEEE Trans. Nucl. Sci. **57** (2010) 1492.
- 3 T. Itoh, T. Yanagida, M. Kokubun, M. Sato, R. Miyawaki, K. Makishima, T. Takashima, T. Tanaka, K. Nakazawa, T. Takahashi, N. Shimura, and H. Ishibashi: Nucl. Inst. Methods Phys. Res., Sect. A **579** (2007) 239.
- 4 S. Moriuchi, M. Tsutsumi, and K. Saito: Jpn. J. Heal. Phys. **44** (2009) 122.
- 5 J. Glodo, Y. Wang, R. Shawgo, C. Brecher, R. H. Hawrami, J. Tower, and K. S. Shah: Phys. Procedia **90** (2017) 285.
- 6 S. E. Derenzo, M. J. Weber, E. Bourret-Courchesne, and M. K. Klintonberg: Nucl. Inst. Methods Phys. Res., Sect. A **505** (2003) 111.
- 7 C. W. E. van Eijk: Nucl. Inst. Methods Phys. Res., Sect. A **460** (2001) 1.
- 8 A. Watanabe, A. Magi, M. Koshimizu, A. Sato, Y. Fujimoto, and K. Asai: Sens. Mater. **33** (2021) 2251.
- 9 S. Arai, M. Koshimizu, Y. Fujimoto, T. Yanagida, and K. Asai: Nucl. Inst. Methods Phys. Res., Sect. A **954** (2020) 161632.
- 10 M. Koshimizu, G. H. V. Bertrand, M. Hamel, S. Kishimoto, R. Haruki, F. Nishikido, T. Yanagida, Y. Fujimoto, and K. Asai: Jpn. J. Appl. Phys. **54** (2015) 102202.
- 11 M. Koshimizu, T. Yanagida, R. Kamishima, Y. Fujimoto, and K. Asai: Sens. Mater. **31** (2019) 1233.
- 12 M. Koshimizu, N. Kawano, A. Kimura, S. Kurashima, M. Taguchi, Y. Fujimoto, and K. Asai: Sens. Mater. **33** (2021) 2137.
- 13 A. Horimoto, N. Kawano, D. Nakauchi, H. Kimura, M. Akatsuka, and T. Yanagida: Sens. Mater. **32** (2020) 1395.
- 14 D. Shiratori, Y. Isokawa, N. Kawaguchi, and T. Yanagida: Sens. Mater. **31** (2019) 1281.
- 15 D. K. Choi: Sens. Mater. **27** (2015) 11.
- 16 D. Shiratori, T. Kato, D. Nakauchi, N. Kawaguchi, and T. Yanagida: Sens. Mater. **33** (2021) 2171.
- 17 H. Kimura, T. Kato, D. Nakauchi, N. Kawaguchi, and T. Yanagida: Sens. Mater. **33** (2021) 2187.
- 18 P. Kantupitim, M. Akatsuka, D. Nakauchi, T. Kato, N. Kawaguchi, and T. Yanagida: Sens. Mater. **32** (2020) 1357.
- 19 H. Fukushima, D. Nakauchi, N. Kawaguchi, and T. Yanagida: Sens. Mater. **31** (2019) 1273.
- 20 J.-L. Boulnois: Lasers Med. Sci. **1** (1986) 47.
- 21 R. Weissleder: Nat. Biotechnol. **19** (2001) 316.
- 22 C. Amiot, S. Xu, S. Liang, L. Pan, and J. Zhao: Sensors **8** (2008) 3082.
- 23 K. Soga, T. Tsuji, F. Tashiro, J. Chiba, M. Oishi, K. Yoshimoto, Y. Nagasaki, K. Kitano, and S. Hamaguchi: J. Phys. Conf. Ser. **106** (2008) 012023.
- 24 A. S. Beddar, T. R. Mackie, and F. H. Attix: Phys. Med. Biol. **37** (1992) 1901.
- 25 J. Archer, L. Madden, E. Li, M. Carolan, and A. Rosenfeld: Biomed. Phys. Eng. Express **4** (2018) 044003.
- 26 H. Fukushima, M. Akatsuka, H. Kimura, D. Onoda, D. Shiratori, D. Nakauchi, T. Kato, N. Kawaguchi, and T. Yanagida: Sens. Mater. **33** (2021) 2235.
- 27 M. Akatsuka, H. Kimura, D. Onoda, D. Shiratori, D. Nakauchi, T. Kato, N. Kawaguchi, and T. Yanagida: Sens. Mater. **33** (2021) 2243.
- 28 Y. Fujimoto, T. Yanagida, T. Kojima, M. Koshimizu, H. Tanaka, and K. Asai: Sens. Mater. **28** (2016) 857.
- 29 M. Akatsuka, D. Nakauchi, T. Kato, N. Kawaguchi, and T. Yanagida: Sens. Mater. **32** (2020) 1373.
- 30 G. Okada, N. Kawaguchi, and T. Yanagida: Sens. Mater. **29** (2017) 1407.
- 31 T. Yanagida, Y. Fujimoto, H. Yagi, and T. Yanagitani: Opt. Mater. **36** (2014) 1044.
- 32 T. Yanagida, Y. Fujimoto, S. Ishizu, and K. Fukuda: Opt. Mater. **41** (2015) 36.
- 33 K. Okazaki, D. Onoda, H. Fukushima, D. Nakauchi, T. Kato, N. Kawaguchi, and T. Yanagida: J. Mater. Sci. Mater. Electron. **32** (2021) 21677.
- 34 Y. Fujimoto, D. Nakauchi, T. Yanagida, M. Koshimizu, and K. Asai: Sens. Mater. **33** (2021) 2147.
- 35 T. Yanagida, K. Kamada, N. Kawaguchi, Y. Fujimoto, K. Fukuda, Y. Yokota, V. Chani, and A. Yoshikawa: Nucl. Inst. Methods Phys. Res., Sect. A **652** (2011) 256.
- 36 C. Zhang, L. Zhang, Z. Wei, C. Zhang, Y. Long, Z. Zhang, H. Zhang, and J. Wang: Opt. Lett. **31** (2006) 1435.

- 37 B. Yan and X. Q. Su: *Opt. Mater.* **29** (2007) 547.
- 38 Y. Fujimoto, T. Yanagida, Y. Yokota, V. Chani, V. V. Kochurikhin, and A. Yoshikawa: *Nucl. Inst. Methods Phys. Res., Sect. A* **635** (2011) 53.
- 39 D. Nakauchi, G. Okada, N. Kawaguchi, and T. Yanagida: *J. Mater. Sci. Mater. Electron.* **28** (2017) 6972.
- 40 D. Nakauchi, G. Okada, N. Kawaguchi, and T. Yanagida: *Jpn. J. Appl. Phys.* **57** (2018) 100307.
- 41 M. Akatsuka, Y. Usui, D. Nakauchi, G. Okada, N. Kawaguchi, and T. Yanagida: *Sens. Mater.* **30** (2018) 1525.
- 42 T. Yanagida, K. Kamada, Y. Fujimoto, H. Yagi, and T. Yanagitani: *Opt. Mater.* **35** (2013) 2480.
- 43 T. Yanagida, Y. Fujimoto, T. Ito, K. Uchiyama, and K. Mori: *Appl. Phys. Express* **7** (2014) 062401.
- 44 L. Yang, C. Wang, Y. Dong, N. Da, X. Hu, D. Chen, and J. Qiu: *Opt. Express* **13** (2005) 10157.
- 45 K. Oka, H. Unoki, H. Shibata, and H. Eisaki: *J. Cryst. Growth* **286** (2006) 288.
- 46 J. Lu, J. Lu, T. Murai, K. Takaichi, T. Uematsu, K. Ueda, H. Yagi, T. Yanagitani, and A. A. Kaminskii: *Jpn. J. Appl. Phys.* **40** (2001) L1277.
- 47 S. Kamimura, C.-N. Xu, H. Yamada, N. Terasaki, and M. Fujihara: *Jpn. J. Appl. Phys.* **53** (2014) 092403.
- 48 M. A. Hernández-Rodríguez, A. D. Lozano-Gorrin, I. R. Martín, U. R. Rodríguez-Mendoza, and V. Lavín: *Sens. Actuators, B* **255** (2018) 970.
- 49 L. Qin, X. Meng, C. Du, Z. Shao, L. Zhu, B. Xu, and H. Zhang: *Jpn. J. Appl. Phys.* **41** (2002) 6018.
- 50 H. Yagi, T. Yanagitani, K. Takaichi, K. Ueda, and A. A. Kaminskii: *Opt. Mater.* **29** (2007) 1258.
- 51 M. Akatsuka, Y. Usui, D. Nakauchi, T. Kato, N. Kawano, G. Okada, N. Kawaguchi, and T. Yanagida: *Opt. Mater.* **79** (2018) 428.
- 52 T. Oya, G. Okada, and T. Yanagida: *J. Ceram. Soc. Jpn.* **124** (2016) 536.
- 53 T. Samanta, A. E. Praveen, and V. Mahalingen: *J. Mater. Chem. C* **6** (2018) 4878.
- 54 M. Akatsuka, T. Yanagida, and N. Kawaguchi: *J. Ceram. Process. Res.* **20** (2019) 280.